Received: 1 February 2016 | Revised: 2 May 2016 | Accepted: 14 May 2016

DOI: 10.1111/cbdd.12794

RESEARCH ARTICLE

WILEY

# Design and synthesis of *N*-benzoyl amino acid derivatives as DNA methylation inhibitors

Davide Garella[1] | Sandra Atlante[2] | Emily Borretto[1] | Mattia Cocco[1] | Marta Giorgis[1] | Annalisa Costale[1] | Livio Stevanato[1] | Gianluca Miglio[1] | Chiara Cencioni[2] | Eli Fernández-de Gortari[3] | José L. Medina-Franco[3] | Francesco Spallotta[2] | Carlo Gaetano[2] | Massimo Bertinaria[1]

[1]Dipartimento di Scienza e Tecnologia del Farmaco, Università degli Studi di Torino, Torino, Italy

[2]Division of Cardiovascular Epigenetics Department of Cardiology, Goethe University, Frankfurt am Main, Germany

[3]Facultad de Química Departamento de Farmacia, Universidad Nacional Autónoma de México, Mexico City, México

**Correspondence**
Davide Garella, davide.garella@unito.it
and
Carlo Gaetano, gaetano@em.uni-frankfurt.de

The inhibition of human DNA Methyl Transferases (DNMT) is a novel promising approach to address the epigenetic dysregulation of gene expression in different diseases. Inspired by the validated virtual screening hit NSC137546, a series of *N*-benzoyl amino acid analogues was synthesized and obtained compounds were assessed for their ability to inhibit DNMT-dependent DNA methylation *in vitro*. The biological screening allowed the definition of a set of preliminary structure–activity relationships and the identification of compounds promising for further development. Among the synthesized compounds, *L*-glutamic acid derivatives **22**, **23**, and **24** showed the highest ability to prevent DNA methylation in a total cell lysate. Compound **22** inhibited DNMT1 and DNMT3A activity in a concentration-dependent manner in the micromolar range. In addition, compound **22** proved to be stable in human serum and it was thus selected as a starting point for further biological studies.

**KEYWORDS**
DNA methylation, DNMT inhibitors, docking, epigenetics, structure–activity relationships

Epigenetic modifications play an essential role in the establishment and regulation of cellular differentiation and gene expression.[1,2] DNA methylation is the most stable epigenetic mark in humans.[3] The DNA methylation occurs at the C5 position of the cytosine ring, particularly in a CpG dinucleotide context, through the action of three active DNA methyltransferases (DNMTs): DNMT1, DNMT3A, and DNMT3B. These enzymes catalyze the transfer of a methyl group from *S*-adenosyl-*L*-methionine (SAM) to the C5-cytosine.[4] DNMT1 is responsible for DNA methylation maintenance during cell replication by methylation of newly synthesized DNA strands; however, it was hypothesized that this enzyme can also participate in the *de novo* methylation process.[5] DNMT3A and DNMT3B are responsible for *de novo* DNA methylation being able to methylate both unmethylated and hemimethylated DNA strands.[6,7] Another protein, lacking enzymatic activity, namely DNMT3L, is capable of interacting with DNMT3A and DNMT3B with the consequence of stimulating their catalytic activity.[8]

In human genome, CpG dinucleotides are typically clustered in regions called CpG islands, which are located in the proximal promoter of more than half of all human genes.[9] When promoter CpG islands are methylated, the corresponding gene is repressed because of poor recognition by transcription factors and by other methyl-binding proteins (MBDs) involved in chromatin remodeling and reorganization.[10]

Aberrant DNA methylation, or the failure to maintain the appropriate DNA methylation status, results in the expression of non-optimal level of gene-associated proteins, which could trigger or exacerbate different pathological responses.

  

For instance, in cancer cells,[11] DNA hypermethylation of CpG islands, joined to a global hypomethylation, gives rise to genomic instability and inactivation of cancer-suppressor genes.[12,13] Altered DNA methylation has also been found to regulate synaptic plasticity in postmitotic neurons,[14] and DNMT1 and DNMT3A have been recently proposed as new targets for antipsychotic therapy.[15] Moreover, hypermethylation of DNA sequences has been linked to the onset of cardiac fibrosis.[16]

On these bases, the potential therapeutic application of DNMT inhibitors is nowadays actively studied.[17–19] A number of DNMT inhibitors has been developed. They can be classified into two general subsets: nucleoside and non-nucleoside DNMT inhibitors (Figure 1).

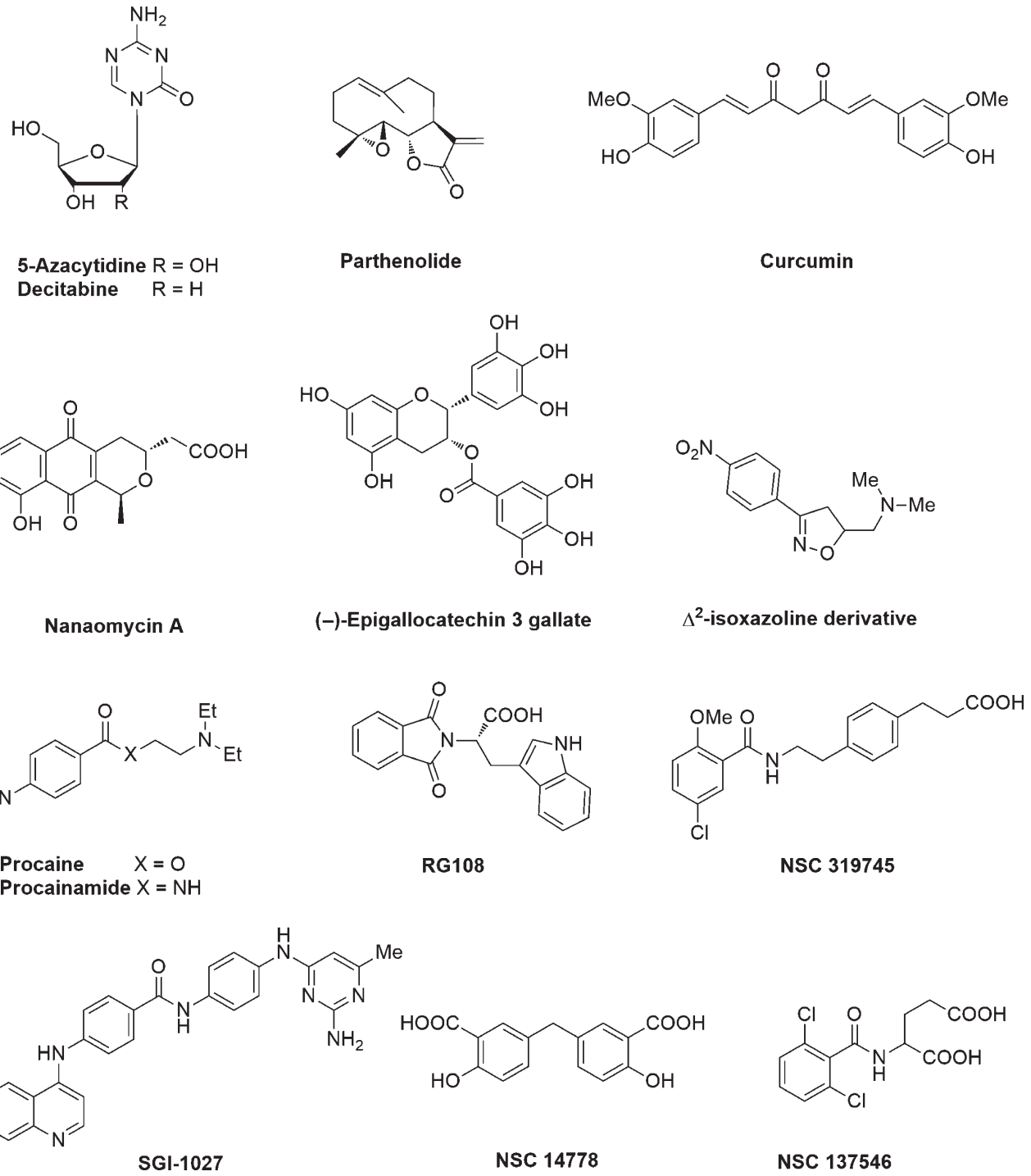


**FIGURE 1** Structure of representative DNMT inhibitors

The first subset comprises 5-azacytidine (5-AZA) and 5-aza-2′-deoxycytidine (decitabine), which are drugs currently employed in the treatment of myelodysplastic syndromes (MDS), chronic myelomonocytic leukemia (CMML), and acute myeloid leukemia (AML). 5-AZA and decitabine are imported into the cell, phosphorylated, and actively integrated in the DNA structure where they act through covalent inhibition of DNMTs. This complex set of events results in an easy onset of resistance and poor reproducibility of action with more than 1000-fold variability in cancer cell lines as demonstrated with decitabine.[20] A second generation of nucleoside analogues is currently under study, among them: 5-fluoro-2′-deoxycytidine, 5,6-dihydro-5-azacytidine (DHAC) and zebularine. The main drawback of these nucleoside DNMT inhibitors is expected to lie in their mechanism of action, similar to that of first generation drugs.

Non-nucleoside DNMT inhibitors are represented by a heterogeneous subset of compounds which can directly inhibit the enzyme. Different compounds have been identified either from natural sources, from screening campaigns, or thanks to synthetic efforts.[17]

Natural products, such as parthenolide, curcumin, and nanaomycin A, are proposed to act by covalent binding to the catalytic cysteine residue in the enzyme pocket.[21–23] A main disadvantage of these compounds could be associated with their lack of selectivity that may reflect in promiscuous binding to other cellular targets.

Hydralazine, procaine, procainamide, isoxazoline derivatives, and the natural compound (-)-epigallocatechin-3-gallate are non-covalent inhibitors. They bind into the enzyme pocket through a complex network of hydrogen bonds in a 2′-deoxycytidine-like binding mode.[24,25] Moreover, thanks to the use of computational techniques and *ad hoc* medicinal chemistry design, an increasing number of small-molecule DNMT inhibitors is now emerging.[26]

A few lead structures have been identified and their rational modulation has been pursued. Most studied model compounds comprise RG108, SGI-1027, NSC14778, NSC319745, and their analogues, which act by competing with SAM or with DNA strand for binding into the respective enzymatic site.[27–32] Furthermore, compounds such as NSC14778 are being used as starting point of computer-assisted drug repurposing of novel hypomethylating agents.[33]

So far, the therapeutic development of non-nucleoside DNMT inhibitors was hampered by the relatively poor inhibitory activity, the lack of isoform selectivity, and a significant cytotoxicity. Therefore, new potent and selective DNMT inhibitors are urgently needed.

Recently, virtual screening of the National Cancer Institute (NCI) compounds library allowed the identification of a glutamic acid derivative, namely NSC137546 (Figure 1), as a potential DNMT1 inhibitor. Of note, in the previous study, the stereochemistry of tested NSC137546 was not defined. This virtual screening hit showed a moderate selective inhibition of DNMT1 versus DNMT3B at 100 $\mu$M concentration. As the virtual screening was conducted at the substrate-binding site of DNMT1, it was hypothesized that the active compound binds into this pocket, although this was not experimentally checked.[32] Indeed, currently there is not reported a crystallographic structure of NSC137546 bound to DNMT that provide evidence for the actual binding site. Actually, for most of the small-molecule DNMT inhibitors described to date, the experimental binding site remains unknown. However, molecular docking has been helpful to propose binding models that require, of course, experimental validation. Inspired by the chemical structure of NSC137546, we decided to explore the chemistry of the *N*-benzoyl amino acidic scaffold with the aim of improving DNMT1 activity and of investigating the selectivity against DNMT3A and DNMT3B. As the predicted docking pose of the (S)- and (R)-forms are largely similar, in this work, we selected the (S) stereochemistry to make use of natural amino acids. Therefore, the structure of 1(*S*)-2-(2,6-dichlorobenzamido) pentanedioic acid (**1**), used as the model template, was modulated according to three different approaches (A–C, Figure 2).

Synthesis of derivatives bearing natural aminoacids as the terminal acidic portion (A moiety in Figure 2) was initially considered, to compare a series of sterically homogenous analogues. A first series of 27 compounds was designed (Schemes 1–3). Derivatives **1**–**8** were prepared to explore the structure–activity relationships (SAR) of the A moiety. Compound **9**, the amino analogue of **1**, was synthesized to verify the role of the amide bond (B moiety) in the activity of this class of compounds. Finally, modulation of the aromatic substructure (C moiety), as in derivatives **10**–**27** (Scheme 3), was performed to gain preliminary SAR information concerning the stereo electronic properties of the aromatic ring.

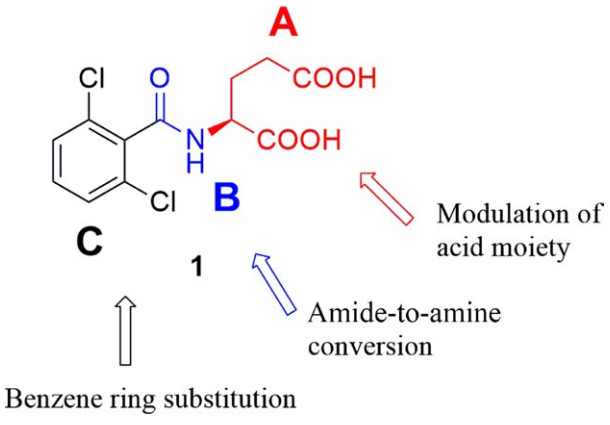


**FIGURE 2** Structure of model compound **1** and chemical modulation strategies applied

The synthesis, the ability of the synthesized compounds to inhibit DNA methylation *in vitro*, and their preliminary SAR are described. The ability of selected compounds to inhibit DNA methylation in cell lysate overexpressing DNMT1, DNMT3A, and DNMT3B isoforms is reported. The action of selected compounds on isolated DNMT1 and DNMT3A enzymes is also reported. Finally, the characterization of the putative binding mode of derivative **22** in the substrate-binding site of DNMT1 and DNMT3A is proposed.

# 1 | METHODS AND MATERIALS

Commercially available reagents and solvents were used without further purification, unless otherwise noted. Reaction progress was monitored by TLC on precoated silica plates (Merk 60 $F_{254}$, 250 $\mu$m thickness), and spots were stained by ceric ammonium molibdate, $KMnO_4$ (0.5 g in 100 mL 0.1 N NaOH), and UV light. Reactions under MW irradiation were carried out in the Synthwave™ oven (Milestone, Shelton, CT, USA). Melting points were measured with a capillary apparatus (Büchi 540). All the compounds were routinely checked by $^1H$ and $^{13}C$ NMR (Bruker Avance 300, Billerica, MA, USA) at 300 and 75 MHz, respectively. Chemical shifts ($\delta$) are given in ppm relative to internal standard TMS (0.00 ppm) or residual solvent peaks ($CDCl_3$ = 7.26 ppm, MeOD = 3.31 ppm, DMSO-$d_6$ = 2.50 ppm and $D_2O$ = 4.79 ppm). $^1H$ NMR coupling constants (*J*) are reported in Herz (Hz) and multiplicity is indicated as follow: s, singlet; bs, broad singlet; d, doublet; dd, doublet of doublet; t, triplet; m, multiplet; Im, imidazole ring; Ph, phenyl ring. Low-resolution mass spectra were recorded on Finnigan-Mat TSQ-700 in chemical ionization (CI) using isobutane. ESI-MS spectra were recorded on a Micromass Quattro micro™ API (Waters, Milford, MA, USA). The purification was performed by flash chromatography (CombiFlash Rf® Teledyne ISCO) on appropriate columns (silica gel). Anhydrous sodium sulfate was used as drying agent for the organic phases. Organic solvents were removed under vacuum at 30 °C. Purity of compounds was checked by UHPLC (PerkinElmer, Waltham, MA, USA) Flexar 15, equipped with UV-Vis diode array detector using an Acquity UPLC CSH Phenyl-Hexyl 1.7 $\mu$m 2.1 × 50 mm column (Waters, Milford, MA, USA) and $H_2O/CH_3CN$ containing 0.1% $CF_3COOH$ and $H_2O/CH_3OH$ containing 0.1% $CF_3COOH$ solvent systems. Detection was performed at $\lambda$ = 200, 215, and 254 nm. The analytical data confirmed that the purity of the products was ≥ 95%. Detailed synthetic procedures are fully described in Supporting Information. Characterization data of **10**–**14**, **16**, **22**, **24**,[34] **15**,[35] **18**,[36] **19**,[37] **21**,[38] are in agreement with those reported.

## 1.1 | Chemistry

### 1.1.1 | General procedure for the synthesis of compounds 1–6, 10–27

Carboxylic acid (2.6 mmol, 1 eq) was solubilized in $SOCl_2$ (22 mmol, 8.5 eq) and irradiated under pressure in a microwave oven (5 bar, $N_2$) at 120 °C for 1.5 h. The solvent was removed under reduced pressure, and the residual oil was solubilized in 1,4-dioxane (5 mL) and added dropwise to a stirring solution of appropriate aminoacid (2.6 mmol) and $Na_2CO_3$ (6.5 mmol) in water (5 mL). The mixture was stirred overnight at room temperature, poured in 1N HCl (40 mL), and extracted with EtOAc (3 × 20 mL). The combined organic layers were washed with brine, dried with anhydrous $Na_2SO_4$, and concentrated under reduced pressure. The residue was triturated with $CH_2Cl_2$ (about 30 mL), and the obtained precipitate was filtered. The product was purified (when required) by flash chromatography (CombiFlash, gradient $CH_2Cl_2$/MeOH 0.1% $CF_3COOH$).

### 1.1.2 | General procedure for the synthesis of compounds 7 and 8

To the compound **3**, (500 mg, 1.6 mmol) solubilized in THF (5 mL) was added DCC (453 mg, 2.2 mmol). The mixture was stirred overnight at room temperature. The mixture was filtered, and the filtrate was partially concentrated under reduced pressure. The appropriate amine (isopropyl amine or benzylamine, 1.6 mmol) was added to the residue, and the mixture was stirred neat (overnight) at room temperature. The solution was poured in water and extracted with $Et_2O$ (1 × 20 mL). The pH was adjusted to 1–2 with 1N HCl, and the aqueous phase was extracted with EtOAc (3 × 20 mL). The organic phases were washed with brine, dried, filtered, and concentrated under reduced pressure to obtain the desired compound without any further purification.

### 1.1.3 | General procedure for the synthesis of (*S*)-Sodium-2-((2,6-dichlorobenzyl)aminopentanedioate) (9)

*L*-glutamic acid (600 mg, 4.0 mmol) and NaOH (320 mg, 8.0 mmol) were solubilized in $H_2O$/MeOH 1:1 (20 mL). 2,6-Dichlorobenzaldehyde (700 mg, 4.0 mmol) was added, and the mixture was stirred at room temperature for 2 h. $NaBH_4$ (227 mg, 6.0 mmol) was added portionwise, and the mixture was stirred overnight at room temperature. The pH of the mixture was adjusted to 5–6 adding acetic acid. After stirring for further 45 min, the solvent was completely removed and the sticky mass was treated with

EtOH (30 mL) to obtain the precipitation of a white solid which was filtered and dried to afford the final compound **9** as a white solid.

## 1.2 | Biology

### 1.2.1 | Total DNMT activity assay

All compounds were screened for total DNMT activity using a DNA methyltransferase (DNMT) activity/inhibitor assay kit (Epigentek, Farmingdale, NY, USA) according to manufacturer's instruction. To measure the effects of the compounds on DNMT activity, 35 $\mu$g of total HaCaT cellular extract freshly prepared in RIPA buffer (Tris–HCl pH 7.4 10 mM, NaCl 150 mM, NP-40 1%, sodium deoxycholate (DOC) 1%, SDS 0.1%, glycerol 0.1%, Protease Inhibitors Cocktail) was incubated with 50 and 100 $\mu$M of the different compounds in DMSO (1% final conc.) or vehicle alone (1% DMSO) at 37 °C for 2 h. As negative control, the lysate was denatured at 100 °C for 30 min. Total lysate was used to avoid the loss of possible coenzyme and complex formation. The amount of methylated DNA, which is proportional to enzyme activity, was colorimetrically detected by a plate reader at 450 nm (EnSpire® Multimode Plate Reader – Perkin Elmer).

### 1.2.2 | Inhibition of DNA methylation in DNMT1, DNMT3A, and DNMT3B overexpressing cell lysates

Compounds **1**, **22** and **24** were tested to evaluate their selectivity on the different DNMT isoforms. To work selectively on DNMT1, DNMT3A, and DNMT3B, HEK293T cells were transfected with the plasmids containing the three different DNMTs' sequences and mock control. Cells were transfected with 2.5 $\mu$g of expression plasmid using Lipofectamine 3000 reagent (Invitrogen, Carlsbad, CA, USA) according the manufacturer's instruction. Plasmids pcDNA3/Myc-DNMT1 (Addgene plasmid # 36939), pcDNA3/Myc-DNMT3A (Addgene plasmid # 35521), and pcDNA3/Myc-DNMT3B1 (Addgene plasmid # 35522) were a gift from Arthur Riggs.[39,40] The presence of exogenous DNMTs was checked by Western blot (not shown), and afterward, the transfected cells were freshly lysed in RIPA buffer as above. Cellular extract of 35 $\mu$g were incubated with selected compounds at different concentration in the 1–150 $\mu$M range (1% DMSO final conc.) or with vehicle alone (1% DMSO) at 37 °C for 2 h. RG108 (Cayman) was used as positive controls, while as negative control, lysates were denatured at 100 °C for 30 min. DNMT activity was detected by DNMT activity/inhibitor assay kit (Epigentek). Data are presented as means ± SD; each compound was tested at least three times.

### 1.2.3 | Inhibition of DNMT1 and DNMT3A activity on isolated enzyme

To assess the specific interaction of DNMT inhibitors with DNMT1 or DNMT3A, the activity assay was performed on the immunoprecipitated enzymes after their overexpression. After DNMT transfection, HEK293T cells were freshly lysed in RIPA buffer as described above (supplemented with Protease Inhibitors Cocktail), and DNMT1 and DNMT3A were immunoprecipitated using paramagnetic beads (Ademtech's Bioadembeads) as previously described.[41] Briefly, 600 $\mu$g of transfected cell extract was incubated at 4 °C for 2 h with DNMT antibodies: anti-DNMT1 (6 $\mu$g, mouse, monoclonal; Abcam ,Cambridge, UK) and anti-DNMT3A (6 $\mu$g, mouse, monoclonal; Abcam). Normal mouse IgG (Santa Cruz Biotechnology, Inc., Dallas, TX, USA) was used as immunoprecipitation control. Then, the immunocomplexes were incubated at 4 °C for 2 h with 60 $\mu$L of paramagnetic beads. All the immunoprecipitation steps have been performed on ice to preserve the enzymatic activity. After elution, the enriched enzymes were incubated with compounds **1** or **22** at 100 $\mu$M (1% DMSO final conc.) or vehicle alone (1% DMSO) at 37 °C for 2 h. RG108 (Cayman) was used as reference, while as negative control, lysates were denatured at 100 °C for 30 min. DNMT activity was detected by DNMT activity/inhibitor assay kit (Epigentek). Data are presented as means ± SD; each compound was tested at least three times. Western blotting analysis was performed, according to standard procedure, to check the immunoprecipitation.

### 1.2.4 | Stability of compound 22 in pH 7.4 phosphate-buffered solution

A stirred solution of compound **22** in pH 7.4 phosphate-buffered solution (final concentration 2 mg/mL) was maintained at 37 ± 0.5 °C for 48 h. At different time intervals, 100 $\mu$L of this solution was withdrawn, diluted to 1 mL with methanol containing 1% $CF_3COOH$, and 5 $\mu$L of the resulting solution was analyzed by RP-UHPLC using a Flexar UHPLC (Perkin Elmer) equipped with a Flexar Solvent Manager 3-CH-Degasser, a Flexar-FX UHPLC autosampler, a Flexar-FX PDA UHPLC Detector, a Flexar-LC Column Oven, and a Flexar-FX-15 UHPLC Pump. The analytical column was an Acquity CSH™ (2.1 × 100 mm, 1.7 $\mu$m particle size) (Waters) column. The samples were analyzed using an isocratic method employing a mobile phase consisting of methanol/water (90/10) containing 0.1% trifluoroacetic acid (flow rate 0.6 mL/min). The column effluent was monitored at $\lambda$ = 220 nm referenced against a $\lambda$ = 360 nm wavelength. Quantification was performed using calibration curves of compound **22** chromatographed under the same conditions.

The linearity of the calibration curves was determined in a concentration range of 1–3 mg/mL ($r^2 > 0.98$). Data analysis was performed using Chromera Manager (Perkin Elmer). All experiments were run in triplicate.

#### 1.2.5 | Stability of compound 22 in human serum

A solution of compound **22** (20 mg/mL) in methanol was added to human serum (sterile-filtered from human male AB plasma; Sigma-Aldrich, Saint Louis, MO, USA) preheated at 37 °C to obtain a final concentration of 2 mg/mL. The resulting solution was incubated at 37 ± 0.5 °C; at appropriate time intervals, 100 μL of the reaction mixture was withdrawn and added to 900 μL of methanol containing 0.1% trifluoroacetic acid in order to deproteinize the serum. The sample was vortexed, and then centrifuged for 5 min at 1500 *g*. The clear supernatant was filtered by Captiva PES 0.2-μm filters (Agilent, Santa Clara, CA, USA) and analyzed by RP-UHPLC.

HPLC analyses were performed as indicated above. The samples (1 μL, injection volume) were analyzed using an isocratic method employing a mobile phase consisting of methanol/water (80/20) containing 0.1% trifluoroacetic acid at a flow rate of 0.2 mL/min. The column effluent was monitored at a $\lambda = 220$ nm referenced against a $\lambda = 360$ nm wavelength. Quantification was performed as indicated above. All experiments were run in triplicate.

#### 1.2.6 | Molecular docking

All flexible ligand docking and scoring calculations were performed with ICM-Pro, version 3.8–4. ICM is based on Monte Carlo optimization of the ligand internal co-ordinates in the space of pocket grid potential maps. The crystallographic structures of DNMT1 (PDB ID: 3PTA) and DNMT3A (PDB ID: 2QRV) were employed. Before docking, the structures of the proteins were prepared using ICM using default settings. To ensure the convergence of the Monte Carlo algorithms, three different cycles were performed for each docked ligand. For the best ten poses, a manual clustering was performed and the docked poses were checked visually. Visualizations and analysis of the protein–ligand complexes were conducted with ICM. The 2D interaction diagram was generated with the MOLECULAR OPERATING ENVIRONMENT (MOE) software, version 2014.09.[42]

### 1.3 | Statistics

Data were collected and analyzed blindly by an observer. Results were expressed as mean ± SD of at least three experiments performed in triplicate. Statistical significance was evaluated by ANOVA and Bonferroni post hoc test (Prism 5, GraphPad Software, La Jolla, CA, USA). Differences were judged statistically significant when $p < 0.1$.

## 2 | RESULTS AND DISCUSSION

### 2.1 | Chemistry

Compound **1** and the analogues **2–6**, modified in the acidic moiety, were synthesized according to the procedure reported in Scheme 1. 2,6-Dichlorobenzoic acid was converted into the corresponding acyl chloride irradiating under pressure (5 bar, $N_2$) in a microwave oven at 120 °C using $SOCl_2$ for 1.5 h. This procedure allowed the use of a parallel chemistry approach generating five acyl chloride derivatives in a single run in almost quantitative yields. After $SOCl_2$ evaporation, the crude product was added dropwise to a stirring solution of the appropriate (S)-amino acid in water using $Na_2CO_3$ as the base. The mixture was stirred at room temperature to afford compounds **1–6** in 40–72% non-optimized yields (Scheme 1). The use of water, as the preferred solvent, allowed for amino acids dissolution, but surely affected the reaction yield. Nevertheless, it avoided the use of polar aprotic solvents (e.g. DMF) which could complicate isolation and purification of the final compounds. Compounds **7** and **8** were synthesized by coupling of **1** with 2-propylamine or benzylamine using dicyclohexylcarbodiimide (DCC) in THF in 50% and 55% yield, respectively (Scheme 1). The structural identity of compounds **7** and **8** was supported by 2D-NMR spectra. For both compounds, the 2D-COSY experiments allowed to discriminate the proton in position 2 from the chiral proton in position 4. The 2D-HMBC experiments showed the correlation of the chiral proton with both the amide carbon atoms, confirming that the new amide bond was formed at the alpha acid (see Supporting Information).

The amino derivative **9** was obtained in 70% yield via reductive amination of 2,6-dichlorobenzaldehyde with *L*-glutamic acid and $NaBH_4$ (Scheme 2).

Derivatives **10–27** (Scheme 3) were synthesized by reaction of *L*-glutamic acid or 4-aminobutanoic acid with the appropriately substituted benzoyl chloride using the expeditious protocol previously developed for the synthesis of compounds **1–6**.

### 2.2 | Biological activity

#### 2.2.1 | Inhibition of total DNA methylation

The ability of the newly synthesized compounds to inhibit DNA methylation was evaluated on HaCaT total cell lysate

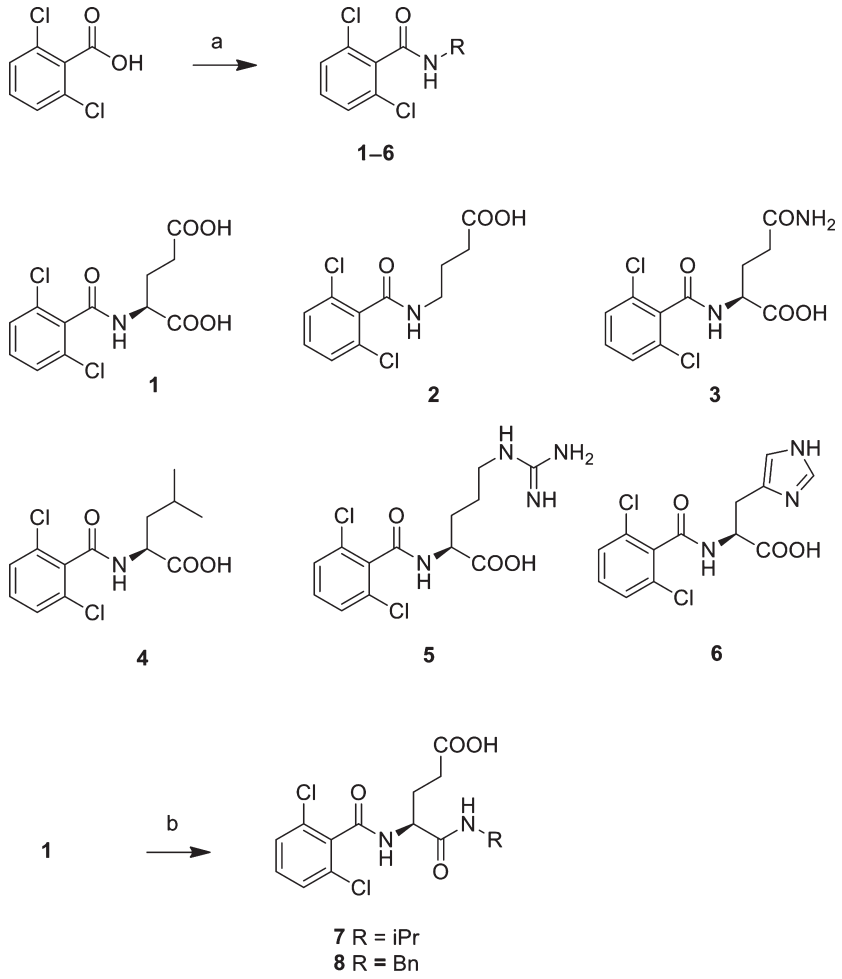


**SCHEME 1** Synthesis of 2,6-dichlorobenzoyl aminoacid derivatives **1**–**8**. Reagents and conditions. (a) (i) $SOCl_2$, MW irradiation 120 °C, $N_2$ (5 bar), 1.5 h; (ii) *L*-amino acid, $Na_2CO_3$, $H_2O$, RT, 12 h. (b) (i) DCC, THF, RT, 12 h; (ii) R-$NH_2$, RT, 12 h

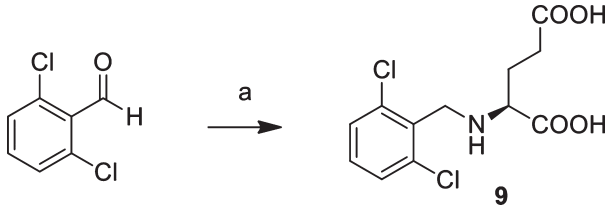


**SCHEME 2** Synthesis of compound **9**. Reagents and conditions. (a) (i) *L*-glutamic acid, NaOH, $H_2O$/MeOH 1/1, RT, 2 h; (ii) $NaBH_4$, RT, 12 h

in order to avoid the loss of possible coenzyme(s) and complex formation. Compounds were incubated at either 100 or 50 $\mu$M for 2 h at 37 °C in a freshly obtained cell lysate. The use of two different concentrations of test compounds was chosen to overcome cellular variability and to afford reliable results, thus avoiding the identification of false-positive hits.

The amount of methylated DNA was quantified using the EpiQuik DNA methyl transferases activity/inhibition assay in comparison with vehicle-treated (DMSO 1%) cell lysate. Results, expressed as the percentage of the residual DNA methylation, are reported in Table 1. Vehicle alone had no effect on DNA methylation in our test system. We would like to point out that many studies highlighted that, depending on the experimental conditions of the enzymatic assay, the inhibitory potency can vary greatly for the same compound; critical factors are the DNA methyltransferase employed, the method of detection, the concentration of the cofactor, and the nature of the DNA duplex used as the substrate.[43]

The ability of synthesized compounds to inhibit total DNA methylation, although initially studied only at two fixed concentrations (100 and 50 $\mu$M), was helpful to draw preliminary SAR indications and to address future chemical modulation of this class of compounds.

Compound **1** (100 $\mu$M) significantly decreased DNA methylation by 39 ± 12% ($p < 0.05$). Removal of the α-carboxylic group (**2**) afforded an inhibition of DNA methylation (40 ± 2%; $p < 0.05$) comparable to that showed by **1**. Both **1** and **2** were ineffective when tested at 50 $\mu$M (Table 1). Conversion of α-COOH into a substituted amide gave compounds **7** and **8**, showing no significant ability to prevent DNA methylation under our assay conditions. The obtained

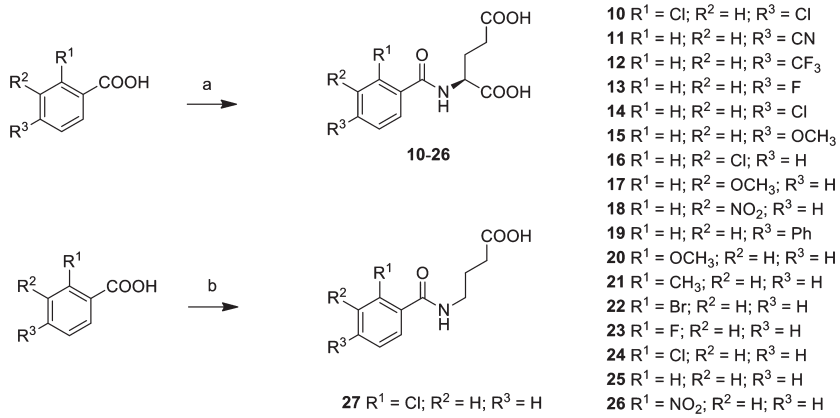


**SCHEME 3** Synthesis of compounds **10**–**27**. Reagents and conditions. (a) (i) $SOCl_2$, MW irradiation 120 °C, $N_2$ (5 bar), 1.5 h; (ii) *L*-glutamic acid, $Na_2CO_3$, $H_2O$, RT, 12 h. (b) (i) $SOCl_2$, MW irradiation 120 °C, $N_2$ (5 bar), 1.5 h; (ii) 4-aminobutanoic acid, $Na_2CO_3$, $H_2O$, RT, 12 h

**TABLE 1** Ability of compounds **1**–**27** to inhibit total DNA methylation expressed as residual relative DNA methylation

| | Residual DNA methylation (%)[a] (mean ± SD[b]) | | | Residual DNA methylation (%)[a] (mean ± SD[b]) | |
|---|---|---|---|---|---|
| **Compound** | **100 μM** | **50 μM** | **Compound** | **100 μM** | **50 μM** |
| **1** | 61 ± 12[c] | 96 ± 6 | **15** | 72 ± 7 | 82 ± 6 |
| **2** | 60 ± 2[c] | 87 ± 15 | **16** | 75 ± 2 | 89 ± 5 |
| **3** | 99 ± 11 | 122 ± 26 | **17** | 69 ± 3 | 97 ± 2 |
| **4** | 126 ± 29[c] | 96 ± 2 | **18** | 58 ± 3[c] | 92 ± 4 |
| **5** | 90 ± 1 | 98 ± 22 | **19** | 64 ± 11 | 93 ± 6 |
| **6** | 58 ± 7[c] | 104 ± 15 | **20** | 81 ± 2 | 85 ± 5 |
| **7** | 82 ± 16 | 118 ± 1[c] | **21** | 60 ± 5[d] | 86 ± 18 |
| **8** | 94 ± 39 | 90 ± 17 | **22** | 45 ± 1[c] | 63 ± 16[d] |
| **9** | 63 ± 1[d] | 111 ± 2 | **23** | 51 ± 9[c] | 68 ± 3[d] |
| **10** | 116 ± 9 | 108 ± 36 | **24** | 68 ± 21[d] | 65 ± 1[d] |
| **11** | 85 ± 20 | 122 ± 16 | **25** | 74 ± 4 | 95 ± 10 |
| **12** | 72 ± 23 | 100 ± 1 | **26** | 107 ± 10 | 103 ± 11 |
| **13** | 57 ± 4[c] | 106 ± 13 | **27** | 99 ± 14 | 93 ± 5 |
| **14** | 70 ± 6[c] | 100 ± 16 | | | |

ANOVA and Bonferroni post hoc test.

[a]Determined in fresh HaCaT cell lysate using Epiquik DNA methyltransferase activity/inhibition assay.

[b]Data are expressed as percentage of residual-methylated DNA relative to vehicle (DMSO 1%)-treated cell lysate. Results are the mean of at least three independent experiments run in triplicate.

[c]$p < 0.05$ versus vehicle.

[d]$p < 0.1$ versus vehicle.

results indicated that substitution of α-carboxylic group in compound **1** with uncharged and bulky groups (compounds **7** and **8**) is not a promising strategy to improve DNMT inhibition in this series of *L*-glutamic acid derivatives, while the role of free α-COOH needs further studies to be fully elucidated.

The modulation of the γ-carboxylic functionality was then considered. The replacement of this carboxylic group with a carboxyamido group (**3**), or its removal (**4**), resulted in a complete loss of activity (Table 1).

The replacement of the γ-COOH with basic groups furnished compounds **5** and **6** bearing a guanidine and imidazole ring in γ-position, respectively. Results showed that the imidazole derivative **6** could conserve the inhibitory activity (42 ± 7% inhibition; $p < 0.05$) while the strongly basic **5** reflected in a complete loss of activity. This result was not unexpected taking into account that γ-COOH in **1** is negatively charged at pH 7.4, while **5** is positively charged. The imidazole ring in **6** (calculated $pK_a$ 7.08) is also present in a positively charged form for about 32% at pH 7.4. Consequently, its residual ability to decrease DNA methylation could be attributed to other properties of this moiety (e.g. metal-complexing ability or 1,3-prototropic tautomerism). Unfortunately, similarly to derivatives **1** and **2**, compound **6**

did not exert any detectable inhibitory effect at lower concentration (50 $\mu$M; Table 1). These preliminary SARs suggest that a putative electrostatic interaction, rather than just hydrogen bonding, could be involved in the binding of the γ-COOH group of **1** with its target (*vide infra*).

Interestingly, when the amide bond of **1** was reduced to afford the amino derivative **9** (B moiety in Figure 2), a behavior similar to that of the parent compound was found, with inhibition of methylation at 100 $\mu$M (37 ± 1%; $p < 0.1$) and no significant inhibition at 50 $\mu$M.

Based on the preliminary SAR data discussed above with the modification of the acidic and amide moieties (A and B, respectively, in Figure 2), we decided to explore the influence of benzene ring substitution (C moiety) keeping the *L*-glutamic acid side chain present in **1** as the preferred moiety A and the amide group.

Moving one chlorine atom from *ortho*-to-*para* position of benzene ring, to obtain the 2,4-dichloro-substituted compound **10**, afforded an inactive compound. Derivatives **24**, **16**, and **14** bearing one chlorine atom in *ortho*, *meta,* and *para* positions, proved able to slightly reduce DNA methylation at 100 $\mu$M showing a residual methylation of 68 ± 21%, 75 ± 2%, and 70 ± 6%, respectively. Interestingly, the *o*-chloro-substituted compound **24** maintained an inhibitory activity (35 ± 1% inhibition) at the lower concentration, demonstrating an improvement with respect to the reference **1**.

These preliminary SAR data, at two compound concentrations, suggest that substitution of benzene ring with a halogen atom in *ortho* position could afford derivatives with improved efficacy as compared to double halogen substitution.

Use of an electron-donating substituent (i.e. a methoxy group) in either position of benzene ring (compounds **15**, **17**, **20**) did not show an increase in the activity when compared with *o*-Clsubstituted **24**, when compounds where tested at 50 $\mu$M concentration.

In order to obtain more hints about the benzene ring substitution preference, and to verify whether we could further improve the activity of **24**, we synthesized and evaluated a series of compounds (**11**–**13**, **18**, **19**, **21**–**23**, and **26**) bearing substituents endowed with different steric and electronic properties. Among the synthesized compounds, **13** (*p*-F substituted), **22** (*o*-Br substituted), and **23** (*o*-F substituted) showed the most attractive activity, being able to inhibit DNA methylation by 43 ± 4% ($p < 0.05$), 55 ± 1% ($p < 0.05$), and 49 ± 9%, ($p < 0.05$), respectively, at 100 $\mu$M. Compounds **22** and **23** were also able to prevent DNA methylation up to a significant extent when tested at 50 $\mu$M (37 ± 16% and 32 ± 3% inhibition). Unsubstituted compound **25** as well as *p*-phenyl-substituted derivative **19** retained a modest activity only at 100 $\mu$M.

Finally, to explore the role of α-COOH group, we combined *o*-chloro substitution (as in **24**) with α-COOH group removal (as in **2**). The obtained derivative **27** proved inactive in our assay, indicating that α-COOH group can play a relevant role in the activity of the *o*-chloro-substituted compound **24**.

### 2.2.2 | Inhibition of DNA methylation in cell lysates selectively over expressing DNMT1, DNMT3A, and DNMT3B

Based on the results of the inhibition of DNA methylation discussed in the previous section, we selected two of the newly designed molecules, **22** and **24**, to further investigate their DNMT inhibition properties. The choice of o-Cl-substituted compound **24**, which is slightly less active than o-F-substituted **23** (at 100 $\mu$M) was performed to directly compare **24** versus **1** over a larger range of concentrations, in order to test the hypothesis that mono-halo-substituted benzoyl amino acids could be better DNMT inhibitors than disubstituted analogues. The new compounds, along with model compound **1**, and RG108 were studied at seven different concentrations (range 1–150 $\mu$M) for their ability to prevent DNA methylation in a HEK293T cell lysate selectively overexpressing DNMT1, DNMT3A, and DNMT3B. All the tested compounds were able to inhibit DNMT1- and DNMT3A-dependent DNA methylation in a concentration-dependent manner with a residual methylation in the 28–49% range in cell lysate overexpressing DNMT1 (Figure 3) and 39–41% in cell lysate overexpressing DNMT3A (Figure 4) at the maximal concentration tested. Interestingly, in this test model, compound **22** proved as active as the reference DNMT inhibitor RG108 maintaining

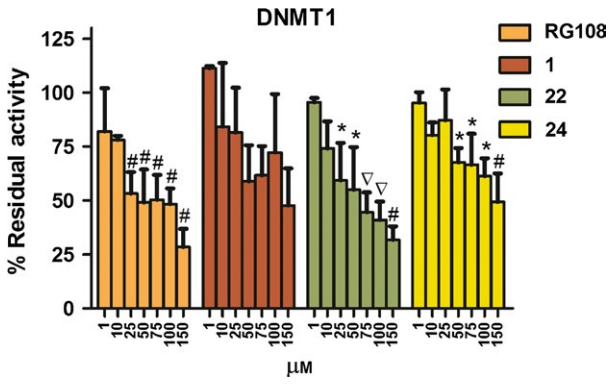


**FIGURE 3** Concentration–response experiments for compounds **1**, **22**, **24**, and reference RG108 showing inhibition of DNA methylation in cell lysate selectively overexpressing DNMT1. HEK293T cells were transfected with plasmids containing DNMT1 sequence and mock control. Fresh cellular extracts were incubated either in the presence of test compounds or with vehicle (1% DMSO) alone for 2 h. The amount of methylated DNA was determined using Epiquik DNA methyltransferase activity/inhibition assay. Data are expressed as percentage of residual-methylated DNA ± SD relative to vehicle (DMSO 1%)-treated cell lysate. Results are the mean of at least three independent experiments run in triplicate. $^{*}p < 0.05$, $^{\nabla}p < 0.01$, and $^{\#}p < 0.001$ versus vehicle-treated lysates; ANOVA and Bonferroni post hoc test

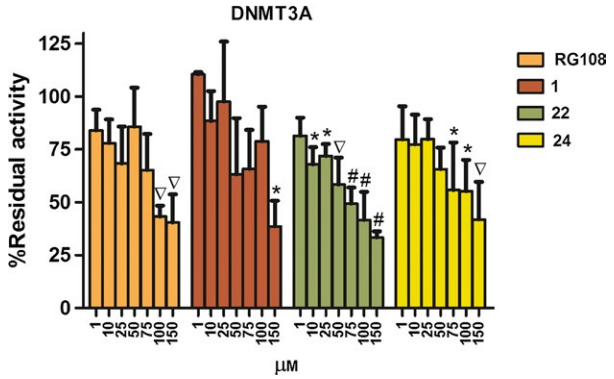


**FIGURE 4** Concentration–response experiments for compounds **1**, **22**, **24**, and reference RG108 showing inhibition of DNA methylation in cell lysate selectively overexpressing DNMT3A. HEK293T cells were transfected with plasmids containing DNMT3A sequence and mock control. Fresh cellular extracts were incubated either in the presence of test compounds or with vehicle (1% DMSO) alone for 2 h. The amount of methylated DNA was determined using Epiquik DNA methyltransferase activity/inhibition assay. Data are expressed as percentage of residual-methylated DNA ± SD relative to vehicle (DMSO 1%)-treated cell lysate. Results are the mean of at least three independent experiments run in triplicate. *$p < 0.05$, $^{\nabla}p < 0.01$, and $^{\#}p < 0.001$ versus vehicle-treated lysates; ANOVA and Bonferroni post hoc test

a significant and encouraging inhibition of DNA methylation up to 25 $\mu$M (**22** = 41 ± 18% versus RG108 = 47 ± 10% inhibition in DNMT1-expressing lysate; **22** = 38 ± 6% versus RG108 = 32 ± 17% inhibition in DNMT3A-expressing lysate). Compounds **1** and **24** proved somewhat less active on both DNMT1 and DNMT3A. All the compounds showed poor or non-significant inhibitory activity in DNMT3B overexpressing cell lysate up to 100 $\mu$M (Table S1).

The obtained data suggest that these compounds are non-selective DNMT1/DNMT3A inhibitors.

### 2.2.3 | Inhibition of DNMT1 and DNMT3A in enzymatic-based assays

To further evaluate the ability of compounds **1**, **22**, and RG108 to act directly on DNMT1 and DNMT3A, the enzymes were overexpressed in HEK293T cells and enriched by immunoprecipitation using the specific antibodies. Enriched enzymes were treated with 100 $\mu$M of compounds **1**, **22**, and RG108; DNA methylation inhibition was measured as above. Results are reported in Table 2. All tested compounds are able to inhibit DNMT1- and DNMT3A-mediated DNA methylation. Compound **22** inhibited both DNMT1 and DNMT3A activity by 42% and 49%, respectively. In this assay, the activity of **1** was very close to that previously reported for NSC137546 (stereochemistry not defined) on recombinant DNMT1.[32] Collectively, these observations suggest that the chemistry of *N*-benzoyl-*L*-glutamic acid derivatives could be further explored to generate mixed DNMT1/DNMT3A inhibitors.

**TABLE 2** Ability of compounds **1**, **22**, and reference compound RG108 to inhibit DNA methylation mediated by isolated DNMT1 and DNMT3A enzymes

| Compound | Residual relative enzymatic activity (%)[a] | |
|---|---|---|
| | DNMT1 (mean ± SD[b]) | DNMT3A (mean ± SD[b]) |
| **1** | 66 ± 15[c] | 61 ± 17[c] |
| **22** | 58 ± 11[d] | 51 ± 13[c] |
| **RG108** | 65 ± 8[c] | 79 ± 3 |

ANOVA and Bonferroni post hoc test.

[a]HEK293T cells were transfected with plasmids containing the different DNMTs' sequences and mock control. Cells were freshly lysed in RIPA buffer, and DNMT1 and DNMT3A were immunoprecipitated using Paramagnetic beads and anti-DNMT1, anti-DNMT3A as antibodies. Normal mouse IgG was used as immunoprecipitation control. All the immunoprecipitation steps have been performed on ice to preserve the enzymatic activity. The immunoprecipitated enzymes were incubated with compounds **1** and **22** at 100 $\mu$M (1% DMSO final conc.) or vehicle alone (1% DMSO) at 37 °C for 2 h. RG108 was used as reference at 100 $\mu$M. DNMT activity was detected by DNMT activity/inhibitor assay kit.

[b]Data are expressed as percentage of residual enzymatic activity relative to vehicle (DMSO 1%)-treated cell lysate ± SD. Results are represented as mean of, at least, three independent experiments run in triplicate.

[c]$p < 0.1$.

[d]$p < 0.05$ versus vehicle.

### 2.2.4 | Docking studies of 22 with DNMT1 and DNMT3A

Molecular docking and other computational techniques have shown to be useful to elucidate the binding mode of experimentally known DNMT1 and DNMT3A inhibitors.[26] To explore the putative protein–ligand interactions of compound **22**, we conducted flexible docking of its structure within the substrate-binding site of the catalytic domain of human DNMT1 and DNMT3A, respectively. Crystallographic structures of DNMT1 (Protein Data Bank, PDB ID: 3PTA)[44] and DNMT3A (PDB ID: 2QRV) were employed.[8] Docking was conducted with the program Internal Coordinates Mechanics (ICM) software.[45] The docking protocol is presented in the Experimental part section. Figure 5 shows a three- and bidimensional (3D and 2D) binding model of **22** in complex with DNMT1. According to this model, the $\gamma$-carboxylate group of **22** makes two important hydrogen bonds with the side chains of Arg1312 and Arg 1310. An additional hydrogen–arene bond is predicted between the phenyl moiety of **22** with Cys1226. The overall position of the compound in the binding pocket and, in particular, the interactions with the catalytic Cys1226, suggests that **22** could inhibit DNMT1 by blocking the substrate-binding site.

Figure 6 depicts the docking model of **22** with DNMT3A. Similar to Figure 5, a 3D model is shown along with a 2D-interaction diagram. In this docking model, the $\alpha$-carboxylate group makes a hydrogen bond with the side chains of Arg887,

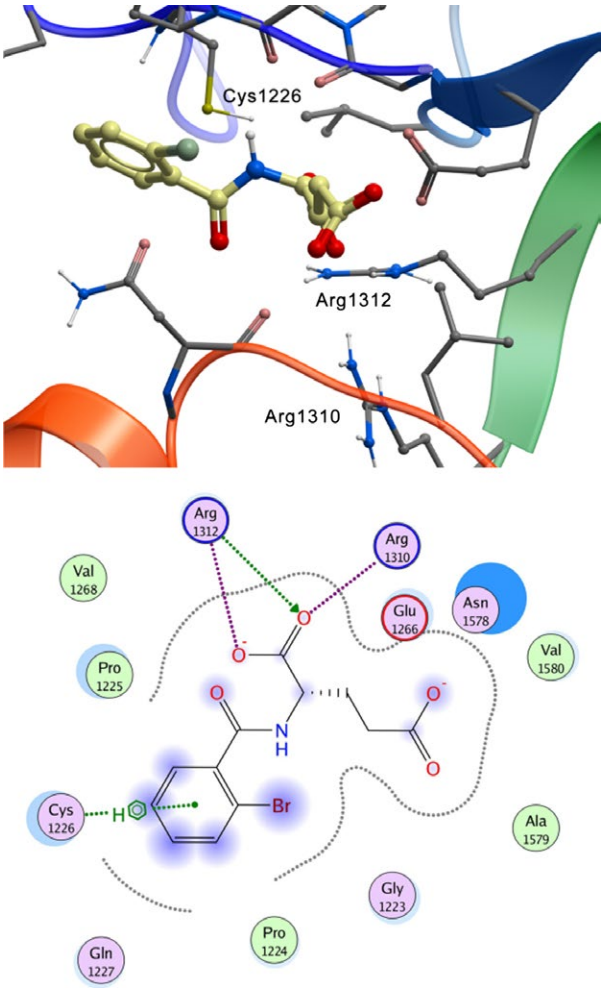


**FIGURE 5** Docking model of compound **22** with the catalytic domain of human DNMT1. The 3D and 2D interaction map show selected amino acid residues of the binding site. Nonpolar hydrogen atoms are omitted for clarity. In the 2D interaction map, green and blue arrows indicate hydrogen bonding to side chain and backbone atoms, respectively. Blue 'clouds' on ligand atoms indicate the solvent-exposed surface area of ligand atoms. Light blue 'halos' around residues indicate the degree of interaction with ligand atoms. The dotted contour reflects steric room for methyl substitution

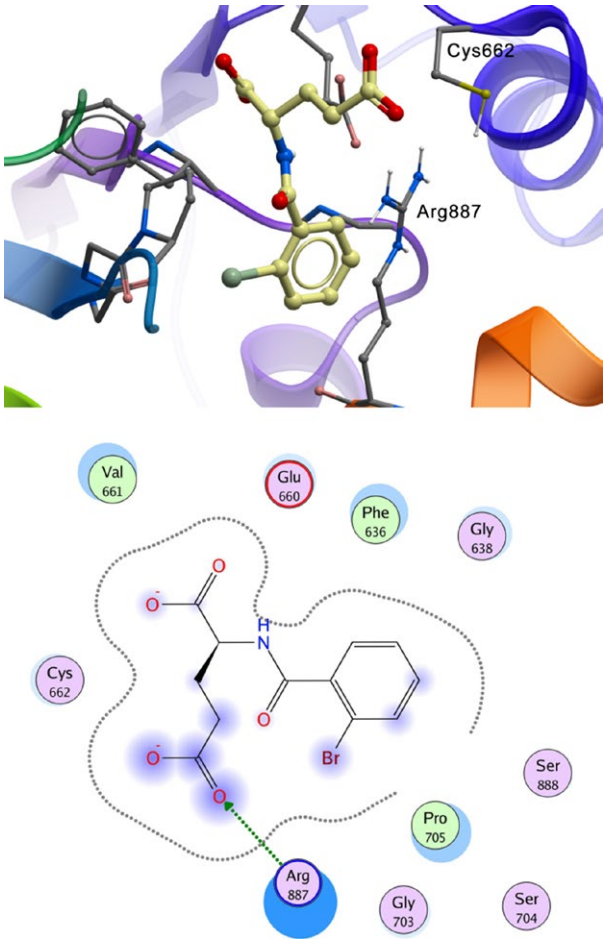


**FIGURE 6** Docking model of compound **22** with the catalytic domain of human DNMT3A. The 3D and 2D interaction map show selected amino acid residues of the binding site. Nonpolar hydrogen atoms are omitted for clarity. In the 2D interaction map, the color coding and symbols are as in Figure 5

but it does not make interactions with the catalytic Cys662. Similar to the binding model with DNMT1, the docking results suggest that **22** could inhibit DNMT3A by blocking the substrate-binding site. In both models, with DNMT1 and DNMT3A, the two carboxylate groups are involved in the formation of hydrogen bonds with residues in the binding site. This result is in overall agreement the SAR discussed above.

### 2.2.5 | Stability of compound 22 under physiological conditions and in human serum

In view of future *in vivo* studies, the chemical stability of **22** under physiological conditions and in human serum was checked. In separate experiments, compound **22** was incubated at 37 °C for 48 h in pH 7.4 phosphate-buffered solution and in human serum (Figure S1) at the concentration of 2 mg/mL. The stability was monitored for 48 h by measuring the compound concentration at different time intervals via RP-UHPLC. Compound **22** was completely stable in both the conditions tested.

## 3 | CONCLUSIONS

Inspired by the structure of the validated hit compound NSC137546, in this work, we synthesized a series of *N*-benzoyl amino acids and explored their ability to inhibit DNMT-dependent total DNA methylation. The SAR derived from this study indicated that the *N*-benzoyl-substituted *L*-glutamic acid scaffold is the minimal requirement for the activity of this class of benzamide derivatives. Ortho-halogeno-substituted compounds **22**, **23**, and **24** emerged as the most interesting hits. In particular, compound **22** inhibited both DNMT1- and DNMT3A-mediated DNA

methylation in a concentration-dependent manner and proved active on both DNMT1 and DNMT3A isolated by immunoprecipitation. Docking studies suggest putative binding to the substrate site of both DNMT isoforms studied. Compound **22** proved to be stable under physiological conditions in human serum, and it is currently being tested in different models of cardiac fibrosis. Results of these studies will be reported in due course.

## ACKNOWLEDGMENTS

This research was supported by funding from the University of Turin, Ricerca locale 2013 'quota B' to D. G., and Ricerca locale 2014 and 2015. C.G. and F.S. are partially supported by a grant from LOEWE Cell & Gene Therapy Center (LOEWE-CGT), Goethe University Frankfurt. F.S. is recipient of the LOEWE-CGT grant # III L 5 - 518/17.004 (2013) and funded by the DFG (German Research Foundation), Excellence Cluster Cardio Pulmonary System (ECCPS). E.F.-deG. is grateful to CONACyT for the Ph.D. Fellowship granted # 348291/240072. We also thank the National Autonomous University of Mexico (UNAM), grant PAPIIT IA204016 to JL.M-F and the program 'Nuevas Alternativas de Tratamiento para Enfermedades Infecciosas' (NUATEI-IIB-UNAM) for the acquisition of the software MOE. Authors wish to thank Prof. Giancarlo Cravotto, DSTF, University of Turin, Italy, and Dr. Marco Lucio Lolli, DSTF, University of Turin, Italy, for access to Synthwave™ oven and UHPLC instrumentations. Authors wish to thank Prof. Loretta Lazzarato for mass spectra.

## REFERENCES

[1] A. Bird, *Nature* **2007**, *447*, 396.
[2] S. L. Berger, T. Kouzarides, R. Shiekhattar, A. Shilatifard, *Genes Dev.* **2009**, *23*, 781.
[3] W. Reik, *Nature* **2007**, *447*, 425.
[4] M. G. Goll, T. H. Bestor, *Annu. Rev. Biochem.* **2005**, *74*, 481.
[5] G. D. Kim, J. Ni, N. Kelesoglu, R. J. Roberts, S. Pradhan, *EMBO J.* **2002**, *21*, 4183.
[6] C. Gros, J. Fahy, L. Halby, I. Dufau, A. Erdmann, J. M. Gregoire, F. Ausseil, S. Vispé, P. B. Arimondo, *Biochimie* **2012**, *94*, 2280.
[7] R. Z. Jurkowska, T. P. Jurkowski, A. Jeltsch, *ChemBioChem* **2011**, *12*, 206.
[8] D. Jia, R. Z. Jurkowska, X. Zhang, A. Jeltsch, X. Cheng, *Nature* **2007**, *449*, 248.
[9] R. S. Illingworth, A. P. Bird, *FEBS Lett.* **2009**, *583*, 1713.
[10] A. Fournier, N. Sasai, M. Nakao, P. A. Defossez, *Briefings Funct. Genomics* **2012**, *11*, 251.
[11] J. Fahy, A. Jeltsch, P. B. Arimondo, *Exp. Opin. Ther. Pat.* **2012**, *22*, 1427.
[12] M. Esteller, *N. Engl. J. Med.* **2008**, *358*, 1148.
[13] S. Sharma, T. K. Kelly, P. A. Jones, *Carcinogenesis* **2010**, *31*, 27.
[14] B. Bie, J. Wu, H. Yang, J. J. Xu, D. L. Brown, M. Naguib, *Nat. Neurosci.* **2014**, *17*, 223.
[15] A. Guidotti, D. R. Grayson, *Dialogues Clin. Neurosci.* **2014**, *16*, 419.
[16] H. Tao, J.-J. Yang, K.-H. Shi, Z.-Y. Deng, J. Li, *Toxicology* **2014**, *323*, 125.
[17] A. Erdmann, L. Halby, J. Fahy, P. B. Arimondo, *J. Med. Chem.* **2015**, *58*, 2569.
[18] J. M. Foulks, K. M. Parnell, R. N. Nix, S. Chau, K. Swierczek, M. Saunders, K. Wright, T. F. Hendrickson, K. K. Ho, M. V. McCullar, S. B. Kanner, *J. Biomol. Screen* **2012**, *17*, 2.
[19] N. Martinet, B. Y. Michel, P. Bertrand, R. Benhida, *MedChemComm* **2012**, *3*, 263.
[20] T. Qin, J. Jelinek, J. Si, J. Shu, J. P. Issa, *Blood* **2009**, *113*, 659.
[21] Z. Liu, S. Liu, Z. Xie, R. E. Pavlovicz, J. Wu, P. Chen, J. Aimiuwu, J. Pang, D. Bhasin, P. Neviani, J. R. Fuchs, C. Plass, P.-K. Li, C. Li, T. H.-M. Huang, L.-C. Wu, L. Rush, H. Wang, D. Perrotti, G. Marcucci, K. Chan, *J. Pharmacol. Exp. Ther.* **2009**, *29*, 505.
[22] Z. Liu, Z. Xie, W. Jones, R. E. Pavlovicz, S. Liu, J. Yu, P.-K. Li, J. Lin, J. R. Fuchs, G. Marcucci, C. Li, K. K. Chan, *Bioorg. Med. Chem. Lett.* **2009**, *19*, 706.
[23] D. Kuck, C. Caulfield, F. Lyko, J. L. Medina-Franco, *Mol. Cancer Ther.* **2010**, *9*, 3015.
[24] N. Singh, A. Duecas-Gonzalez, F. Lyko, J. L. Medina-Franco, *ChemMedChem* **2009**, *4*, 792.
[25] W. J. Lee, J.-Y. Shim, B. T. Zhu, *Mol. Pharmacol.* **2005**, *68*, 1018.
[26] J. L. Medina-Franco, O. Mendez-Lucio, A. Dueñas-González, J. Yoo, *Drug Discov. Today* **2015**, *20*, 569.
[27] S. Valente, Y. Liu, M. Schnekenburger, C. Zwergel, S. Cosconati, C. Gros, M. Tardugno, D. Labella, C. Florean, S. Minden, H. Hashimoto, Y. Chang, X. Zhang, G. Kirsch, E. Novellino, P. B. Arimondo, E. Miele, E. Ferretti, A. Gulino, M. Diederich, X. Cheng, A. Mai, *J. Med. Chem.* **2014**, *57*, 701.
[28] S. Asgatay, C. Champion, G. Marloie, T. Drujon, C. Senamaud-Beaufort, A. Ceccaldi, A. Erdmann, A. Rajavelu, P. Schambel, A. Jeltsch, O. Lequin, P. Karoyan, P. B. Arimondo, D. Guianvarch, *J. Med. Chem.* **2014**, *57*, 421.
[29] S. Castellano, D. Kuck, M. Viviano, J. Yoo, F. Lopez-Vallejo, P. Conti, L. Tamborini, A. Pinto, J. L. Medina-Franco, G. Sbardella, *J. Med. Chem.* **2011**, *54*, 7663.
[30] A. Kabro, H. Lachance, I. Marcoux-Archambault, V. Perrier, V. Dore, C. Gros, V. Masson, J.-M. Gregoire, F. Ausseil, D. Cheishvili, N. Bibens Laulan, Y. St-Pierre, M. Szyf, P. B. Arimondo, A. Gagnon, *MedChemComm* **2013**, *4*, 1562.
[31] J. Yoo, S. Choi, J. L. Medina-Franco, *PLoS ONE* **2013**, *8*(4), e62152.
[32] D. Kuck, N. Singh, F. Lyko, J. L. Medina-Franco, *Bioorg. Med. Chem.* **2010**, *18*, 822.
[33] O. Méndez-Lucio, J. Tran, J. L. Medina-Franco, N. Meurice, M. Muller, *ChemMedChem* **2014**, *9*, 560.
[34] L. Rovati, F. Makovec, R. Chiste, P. Senin, Patent, BE 902726 A1 19851016, 1985.
[35] T. Shiokari, S. Ueda, M. Iwata, K. Yukinori, Patent, EP 226304 A1 19870624, 1987.
[36] A. Rosowsky, H. Baader, R. A. Forsch, R. G. Moran, J. H. Freisheim, *J. Med. Chem.* **1988**, *31*, 763.
[37] G. Groth, Patent, WO 2013093007 A1 20130627, 2013.
[38] Y.-J. Xiao, J.-G. Wang, X.-H. Liu, Y.-H. Li, Z.-M. Li, *Gaodeng Xuexiao Huaxue Xuebao* **2007**, *28*, 1280.
[39] Z. X. Chen, J. R. Mann, C. L. Hsieh, A. D. Riggs, F. Chedin, *J. Cell. Biochem.* **2005**, *95*, 902.
[40] H. Li, T. Rauch, Z. X. Chen, P. E. Szabo, A. D. Riggs, G. P. Pfeifer, *J. Biol. Chem.* **2006**, *281*, 19489.
[41] F. Spallotta, C. Cencioni, S. Straino, S. Nanni, J. Rosati, S. Artuso, I. Manni, C. Colussi, G. Piaggio, F. Martelli, S. Valente, A. Mai, M. C. Capogrossi, A. Farsetti, C. Gaetano, *J. Biol. Chem.* **2013**, *288*, 11004.
[42] Molecular Operating Environment (MOE), version 2014.09, Chemical Computing Group Inc., Montreal, Quebec, Canada. Available at http://www.chemcomp.com
[43] D. Guianvarc'h, P. B. Arimondo, *Fut. Med. Chem.* **2014**, *6*, 1237.
[44] J. Song, O. Rechkoblit, T. H. Bestor, D. J. Patel, *Science* **2011**, *331*, 1036.
[45] M. A. C. Neves, M. Totrov, R. Abagyan, *J. Comp. Aided Mol. Des.* **2012**, *26*, 675.

## SUPPORTING INFORMATION

Additional Supporting Information may be found online in the supporting information tab for this article.

**Data S1.** Characterization of compounds **1–9**, **17**, **20**, **23**, **25**-**27**.

**Data S2.** $^{1}H$ and $^{13}C$-NMR spectra of compounds **1–9**, **17**, **20**, **23**, **25**-**27**.

**Table S1.** Ability of compounds **1**, **22**, **24**, and reference compound RG108 to inhibit DNA methylation in cell lysate selectively overexpressing DNMT3B.

**Figure S1.** Stability of compound **22** in human serum.